



# Fabrication of electrospun HPGL scaffolds via glycidyl methacrylate cross-linker: Morphology, mechanical and biological properties



Fernando José Costa Baratéla<sup>a</sup>, Olga Zazuco Higa<sup>a</sup>,  
Esdras Duarte dos Passos<sup>b</sup>, Alvaro Antonio Alencar de Queiroz<sup>c,d,\*</sup>

<sup>a</sup> Biotechnology Center, Institute of Energy and Nuclear Research (IPEN), Av. Professor Lineu Prestes 2242, 05508-000 São Paulo, SP, Brazil

<sup>b</sup> PostGraduate Program in Materials for Engineering, Federal University of Itajubá (UNIFEI), Av. BPS 1303, 37500-903 Itajubá, MG, Brazil

<sup>c</sup> Physics and Chemistry Institute (IFQ), Federal University of Itajubá (UNIFEI), Av. BPS 1303, 37500-903 Itajubá, MG, Brazil

<sup>d</sup> High Voltage Laboratory (LAT-EFEI), Federal University of Itajubá (UNIFEI), Av. BPS 1303, 37500-903 Itajubá, MG, Brazil

## ARTICLE INFO

### Article history:

Received 2 May 2016

Received in revised form 30 August 2016

Accepted 7 December 2016

Available online 11 December 2016

### Keywords:

Hyperbranched polyglycerol

Electrospun scaffolds

Tissue engineering

Electrospinning

Fibroblast cell

## ABSTRACT

Electrospinning is a suitable method to produce scaffolds composed of nanoscale to microscale fibers, which are comparable to the extracellular matrix (ECM). Hyperbranched polyglycerol (HPGL) is a highly biocompatible polyether polyol potentially useful for the design of fibrous scaffolds mimicking the ECM architecture. However, scaffolds developed from HPGL have poor mechanical properties and morphological stability in the aqueous environments required for tissue engineering applications. This work reports the production of stable electrospun HPGL scaffolds (EHPGLS) using glycidyl methacrylate (GMA) as cross-linker to enhance the water stability and mechanical property of electrospun HPGL. The diameter and morphology of the produced EHPGLS were analyzed by scanning electron microscopy (SEM). It was observed that electrical fields in the range of  $0.2 \text{ kV} \cdot \text{cm}^{-1}$  to  $1.0 \text{ kV} \cdot \text{cm}^{-1}$  decrease the average fiber diameter of EHPGLS. The increase in porosity of EHPGLS with GMA concentration indicates the in situ formation of a heterogeneous structure resultant from the phase separation during crosslinking of HPGL by GMA. EHPGLS containing 20% (w/w) GMA concentration possessed highest tensile strength ( $295.4 \pm 11.32 \text{ kPa}$ ), which is approximately 58 times higher than that of non-crosslinked EHPGLS ( $5.1 \pm 2.12 \text{ kPa}$ ). The MTS cell viability results showed that the EHPGLS have no significant cytotoxicity effect on Chinese hamster ovary (CHO-K1) cells. Scanning electron microscopy (SEM) indicates that the cultured BALB/3T3 fibroblasts cells were able to keep contact each other's, thus forming a homogeneous monolayer on the internal surface of the EHPGLS.

© 2016 Elsevier B.V. All rights reserved.

## 1. Introduction

The advances in the manufacture of polymer matrices from a variety of polymeric materials and the overabundance of fabrication techniques in attempts to production of three-dimensional porous matrices for

regeneration of different biological tissues and organs indicates the significance and potential of polymer materials in the development of scaffolds for tissue engineering [1–2]. However, it is to be noted that the degree of clinical success about the polymeric scaffolds depends essentially on the architecture and biocompatibility of the synthetic macromolecule.

In recent years, a variety of dendritic macromolecules (DMs) have been synthesized for the production of scaffolds opening new possibilities for biomedical applications [3–6]. Advantages provided by DMs are the high density of reactive sites on periphery of the macromolecule offering modulation of the crosslinking and porosity that could be combined with their water absorption and wettability, non-toxicity, low immunogenicity and antigenicity regulating the cell response and tissue regeneration [7–8].

Scaffolds based on DMs possessing novel and interesting physical and biological properties already have been applied in regenerative medicine products or are presently being widely investigated [9–11]. Among DMs, hyperbranched polyglycerol (HPGL), a macromolecule synthesized from glycerol belongs to be promising for the production

**Abbreviations:** HPGL, Hyperbranched polyglycerol; EHPGLS, Electrospun HPGL scaffolds; GMA, Glycidyl methacrylate; E, Elastic modulus; USP-HDPE, United States Pharmacopeia High Density Polyethylene; BALB/3T3, albino house mouse embryo cultures cells; FBs, Fibroblasts cells; SEM, Scanning Electron Microscopy; ECM, Extracellular Matrix; TE, Tissue Engineering; TE, tissue engineering; PGL, Polyglycerol core;  $M_n$ , Numeric Molecular Weight;  $M_w$ , Ponderal Molecular Weight; NMR, Nuclear Magnetic Resonance; FTIR (ATR), Fourier Transform Infrared (Attenuated Total Reflectance); DMAP, 4-(*N,N*-dimethylamino)pyridine; DMF, Dimethylformamide; UV, Ultraviolet spectroscopy; PBS, Phosphate-Buffered Saline; GD, Glutaraldehyde; EWC, Equilibrium Water Content;  $D_c$ , Diffusion Coefficient; *GF*, Gel Fraction; ANOVA, Analysis of Variance.

\* Corresponding author at: Institute of Physics and Chemistry – IFQ, High Voltage Laboratory – LAT-EFEI, Federal University of Itajubá – UNIFEI, Av. BPS 1303, CEP: 37500-903 Itajubá, MG, Brazil.

E-mail address: [alencar@unifei.edu.br](mailto:alencar@unifei.edu.br) (A.A.A. de Queiroz).

of scaffolds for tissue engineering, despite the fact that its potential of becoming a high value product of renewable source that has not yet been fully estimated. The biocompatible and mechanical properties of scaffolds based on HPGL determine their applications in medicine that range from biosensors to wound dressings [12–15].

Recently, attempts have been made to produce polymer scaffolds for medical vascular grafts through electrospinning technique [16–18]. Electrospinning is a process that produces a nonwoven fibers by pushing a millimeter diameter polymer liquid jet through a nozzle with a high electrical field [19]. As a polymer jet is drawn out of the needle orifice, these jets travel downward and become thinner as the solvent evaporates producing nonwoven mesh polymeric fibers at micro/nano-scale in a metallic collecting plate. The electrospinning technique seems to be particularly important since many efforts have been devoted in recent years to explore new skin substitutes and modern wound dressing materials using tissue engineering approaches. Indeed, we recently demonstrated that HPGL is readily electrospun and their derivatives are promising scaffolds for wound dressings [20].

The current trend of burn wound care has been the use of electrospun scaffolds seeded with fibroblasts (FBs) [21–23]. FBs are mesenchymal cells that can be readily cultured in in-vitro conditions and play a significant role in epithelial-mesenchymal interactions, secreting various growth factors and cytokines influencing the epidermal proliferation, differentiation and formation of extracellular matrix [24–26]. Studies have shown that the pre-seeding FBs on a synthetic scaffold prior to implantation are important to overcome the lag phase of cellular growth in the ECM remodeling process and rate of scaffold integration [27–33].

In this study, we hypothesized that electrospun HPGL might provide a suitable scaffold (EHPGLS) for 3D cell culture [13–15,20]. However, when immersed in water EHPGLS swell and collapse into films with a significantly decrease in their surface area, the number of interconnected pores and tensile strength limiting their practical application in soft tissue engineering.

Nowadays, it is well known that the mechanical strength together with the porosity and pore interconnectivity plays an important role in the clinical successful of three-dimensional scaffolds for tissue engineering applications [34–37]. Previous studies have demonstrated that the biological tissue repair is based on the mechanosensitive hypothesis where changes in cell motility and their capacity to form a new extracellular matrix (ECM) appear to be dependent of both, pore size and elastic modulus of the scaffold [38–40].

The purpose of this work was to assess the impact of GMA crosslinker on the EHPGLS descriptor scaffold properties (i.e., morphology, elastic modulus, swelling and cellular viability). To the best of our knowledge a detailed description of the descriptor properties of EHPGLS has not been reported before. Moreover, the produced EHPGLS were characterized using different analytical methods. Finally, after fulfillments of electrospinning conditions for preparation of EHPGLS and their characterization, the utilization of this product as biomaterial for tissue engineering was subjected to FBs adhesion and proliferation studies. The results obtained in this work may be relevant to applications of EHPGLS in medicine as scaffolds for wound healing biomaterials.

## 2. Materials and methods

### 2.1. Materials

All chemicals were purchased from Sigma–Aldrich and were used as received. NaOH (LabSynth). Dulbecco's Modified Eagle Medium (DMEM, Gibco) were used in cytotoxicity test. The DMEM medium was supplemented with 10% (v/v) fetal bovine serum (FBS), 2 mM L-glutamine (Sigma–Aldrich) and 1% (v/v) Gentamicin/Amphotericin B (Sigma–Aldrich, 10,000 units/mL Penicillin, 10 mg/mL Streptomycin and 25 µg/mL Amphotericin B).

### 2.2. Synthesis of HPGL

HPGL was synthesized with a one step process previously described [20,34]. Briefly, a polyglycerol core (PGL) with a molecular weight ( $M_n$ ) of 12 kDa and narrow polydispersity ( $M_w/M_n = 1.46$ ) was synthesized through the reaction of partially deprotonated 1,1,1-tris(hydroxymethyl)propane with glycerol carbonate [20,34]. After neutralization by filtration over cation-exchange resin, the HPGL was purified by precipitation in acetone and subsequently dried for 24 h at 80 °C under vacuum. 400 MHz- $^1\text{H}$  NMR ( $\text{D}_2\text{O}$ , 25 °C):  $\delta$  [ppm]: 3.32–3.84 ( $\text{CH}_2\text{—O—}$ , CH,  $\text{CH}_2$ ). 100 MHz- $^{13}\text{C}$  NMR ( $\text{D}_2\text{O}$ , 25 °C):  $\delta$  [ppm] = 62.60, 62.80 (L1,3), 64.20, 64.41 (T), 70.64–71.40 (L1,4–L1,3), 72.20–72.77 (T, L1,4, L1,3, D), 74.20 (L1,4), 79.80, 81.10 (D), 81.42, 81.58 (L1,3). FTIR (ATR):  $\nu(\text{cm}^{-1}) = 3350$  (O—H), 2870 (C—H), 1066 (C—O—C) and further characteristic peaks at 1458, 1329, 930, 870, 530.

### 2.3. Synthesis of HPGL-GMA macromonomers

The HPGL was functionalized with methacrylate groups after reaction with glycidyl methacrylate (GMA) for the covalent crosslinking of the HGPL chains and formation of the hydrogel [20]. Briefly, HPGL was dissolved in dimethyl sulfoxide (10 mL) and 4-(*N,N*-dimethylamino)pyridine (DMAP) (2.0 g). GMA (1.0 mmol) was added under gentle stirring to obtain a HPGL with GMA substitution degree (SD) of 2.5, 5.0, 10.0 and 20% (w/w). The maximum SD value obtained for incorporation of GMA on HPGL in this work was 20% and appears to be limited by accessibility of the crosslinker agent to secondary hydroxyls on HPGL structure. The HPGL-GMA was re-precipitated three times in diethylether, washed three times with the same solvent and subsequently dried overnight under vacuum at room temperature (25 °C).

HPGL and HPGL-GMA samples were dissolved in  $\text{D}_2\text{O}$  at a concentration of 2–4 µg/mL.  $^1\text{H}$  NMR spectra were recorded with a 400 MHz Bruker NMR spectrometer. The percentage of double bonds (DM) was calculated using Eq. (1) [41]:

$$\text{DM}(\%) = \frac{\sum \left[ \frac{H_a}{3} + \left( \frac{H_b + H_c}{2} \right) + \frac{H_d}{6} \right]}{\left( \frac{H_{\text{HPGL}} - 1}{6} \right)} \quad (1)$$

where  $H_{\text{HPGL}}$  represents H atoms in the HPGL backbone,  $H_a$  represents H atoms in the methyl group,  $H_b$  and  $H_c$  represents the H atoms in methylene group of GMA and  $H_d$  represents the H atoms of hydroxyl group of HPGL.

### 2.4. Production of electrospun HPGL-GMA scaffolds (EHPGLS)

The EHPGLS were prepared by electrospinning from neat 30 wt% HPGL-GMA solution in a mixture of 1:1 v/v methanol and DMF solution. The HPGL solution was placed in a 10 mL glass syringe fitted to a needle with a tip diameter of 0.9 mm. A high electrical field of 0.2–2.0 kV·cm $^{-1}$  was applied to the needle using a high voltage power supply. The ground collection plate of aluminum foil was located at a fixed distance of 20 cm from the needle tip. A syringe pump was used to feed the polymer solution to the needle tip at a feeding rate of 1.5 mL·h $^{-1}$  under UV radiation (200 W UV lamp, 280 nm) to crosslinking HPGL chains by photopolymerization of GMA groups.

The EHPGLS were carefully detached from the collector plate and dried under vacuum for 48 h at room temperature (25 °C) to remove solvent molecules completely. After that, they were soaked in pH 7.4 phosphate-buffered saline (PBS) and then dehydrated by lyophilization.

## 2.5. Physicochemical characterization of EHPGLS

### 2.5.1. EHPGLS morphology

The surface morphology of EHPGLS was characterized prior to and after FBs cell attachment were examined by scanning electron microscopy (SEM). The adhered FBs cells on EHPGLS were fixed using 2.5% (v/v) glutaraldehyde (GD) solution (Sigma-Aldrich) for 24 h, and washed three times with 0.1 M phosphate buffered saline solution (PBS, pH 7.4) to remove the residual GD. The samples were then dried using a graded series of ethanol (70%–80%–90%–95%–100%) at 20 min intervals. After drying by lyophilization, the samples were sputter coated with gold (40 mA) by using a Sputter Coater SCD 050, and examined using a Phillips XL30 scanning electron microscope operated at 15 kV.

### 2.5.2. Scaffold porosity

The porosity of the EHPGLS was measured by pycnometry. Because EHPGLS are hydrophilic, a highly hydrophobic liquid (n-heptane, C<sub>7</sub>H<sub>16</sub>) was used in procedure because it readily penetrated the pores of the matrices and did not induce shrinkage or swelling of the material. The weight of dry EHPGLS was immersed in a pycnometer full of C<sub>7</sub>H<sub>16</sub> for 24 h until no air bubbles were observed emerging from the membranes. The C<sub>7</sub>H<sub>16</sub> impregnated EHPGLS was removed from the pycnometer and the weight of residual C<sub>7</sub>H<sub>16</sub> and pycnometer was measured. Porosities of EHPGLS scaffolds were determined from Eq. (2) [42]:

$$P(\%) = \frac{(W_2 - W_1)}{(\rho V_1)} \cdot 100 \quad (2)$$

where  $W_2$  is the saturation mass of the sample after immersion,  $W_1$  is the initial mass of the sample,  $V_1$  is the volume of the sample prior to immersion in pycnometer filled with C<sub>7</sub>H<sub>16</sub> and  $\rho$  is the density of C<sub>7</sub>H<sub>16</sub> at 25 °C (684 kg/m<sup>3</sup>).

### 2.5.3. Young modulus measurements

Tensile properties (Young's modulus) of EHPGLS were determined using samples cut from electrospun membranes in according to ASTM D-1708 standard, 60 mm in length, 10 mm in width and  $30 \pm 5 \mu\text{m}$  in thickness, at a crosshead speed of 10 mm/min. In order to prevent the grips from direct contact with the EHPGLS membranes, cushion tabs were used. Before measurements the EHPGLS samples were preconditioned at  $37 \pm 1$  °C and  $90 \pm 2\%$  relative humidity (RH). The strength at break and elastic modulus were determined with an Instron Instrument according to ASTM D-882 [43] using a load cell of 100 N at  $5 \text{ mm} \cdot \text{min}^{-1}$  and 20 mm grip distance. At least five measurements were taken, and the average was calculated for each electrospun membrane.

### 2.5.4. Swelling assay and water diffusion

For the swelling assay and water diffusion studies four replicas of pre-weighed dry EHPGLS discs (10 mm in diameter) were immersed in PBS solution pH 7.4 for 72 h at 37 °C. The swollen EHPGLS scaffold discs were periodically removed from PBS, blotted with filter paper, and weighed. The equilibrium water content (EWC), reflecting the maximum amount of water absorbed by EHPGLS samples was gravimetrically calculated through Eq. (3) [44,45]:

$$\text{EWC}(\%) = \frac{(M_s - M_o)}{M_s} \cdot 100 \quad (3)$$

where  $M_s$  and  $M_o$  are the weight of swollen gel at equilibrium and the initial weight of scaffolds, respectively.

The diffusion coefficient ( $D_c$ ) of water through EHPGLS samples was evaluated by following the Eq. (4) [46]:

$$D_c = \pi \left( \frac{h \cdot \alpha}{4 \cdot \text{EWC}} \right)^2 \quad (4)$$

where EWC is swelling of EHPGLS at equilibrium,  $\alpha$  is the slope of the linear part of the swelling curves and  $h$  is the initial thickness of electrospun samples before swelling.

### 2.5.5. Determination of gel fraction (GF) in EHPGLS

A leaching assay was conducted to identify any non-crosslinked EHPGLS and to determine the gel fraction (GF). After swelling assay the non-crosslinked fraction of EHPGLS was supposed to be fully dissolved in the PBS solution pH 7.4 and could be separated from the remaining, EHPGLS-GMA crosslinked and hence insoluble, scaffold matrix ("gel"). This insoluble residue was dried at 80 °C in a vacuum oven until constant weight, followed by determination of its net weight ( $W_d$ ). The ratio of the mass of the insoluble residue divided by the initial mass ( $W_i$ ) of the test sample yields GF of the sample in according to Eq. (5) [47]:

$$\text{GF (hydrogel \%)} = \frac{W_d}{W_i} \cdot 100 \quad (5)$$

where,  $W_i$  is the initial weight of dried EHPGLS and  $W_d$  is the weight of the dried insoluble part of sample after extraction with PBS solution.

## 2.6. Evaluation of biological properties of EHPGLS

### 2.6.1. In vitro cytotoxicity test

To investigate the suitability of the EHPGLS for tissue engineering applications, cytotoxicity studies were performed through the indirect contact method. In the indirect cytotoxicity study, Chinese ovary hamster (CHO-K1, ATCC) cells were used to assess the cytotoxicity of the EHPGLS in according to guidelines of ISO 10993-5 [48]. The CHO cell assay is a sensitive and specific test that can augment both the speed and reliability of the biocompatible properties of synthetic materials and become a standard laboratory tools.

The EHPGLS samples were sterilized by gamma rays from <sup>60</sup>Co (25 kGy) at room temperature (25 °C). The CHO cell culture media (supplemented DMEM) was put in contact with EHPGLS samples at concentration of 1.0 cm<sup>2</sup>/mL and incubated at 37 °C, 5% CO<sub>2</sub> in air for 72 h to obtain the extract media to assess the cytotoxicity of the scaffold as a result of some extractable residual chemical compound or foreign particulates.

CHO cells were routinely cultivated in DMEM media at 37 °C and 5% CO<sub>2</sub> to confluency at which point they were trypsinised and seeded into 96 well plates at a density of  $1.0 \cdot 10^4$  cells/mL (100  $\mu\text{L}$ ) and incubated for 24 h at 37 °C. After overnight cultivation, the culture medium was replaced with fresh medium that contained serial dilutions of the extracts of the EHPGLS samples. HDPE (High-density polyethylene) and phenol 0.3% (m/v) in PBS (pH 7.4) solution were used as negative and positive controls, respectively. CHO viability after exposure was determined by MTS assay after addition of 3-(4,5-dimethylthiazol-2-yl)-5-(3-carboxymethoxyphenyl)-2-(4-sulfophenyl)-2H-tetrazolium (MTS)/phenazinemethosulfate (PMS) (20:1) solution. The absorbance of viable CHO cells was measured at 490 nm using a microplate reader. The cytotoxicity index (IC<sub>50</sub>) was estimated by curve interpolation as the biomaterial extract concentration resulting in 50% inhibition of MTS uptake after plotting the mean percentage of surviving cells against the concentration of the extract.

### 2.6.2. Fibroblasts culture

FBs response to EHPGLS was evaluated in vitro against BALB/3T3 cells line. BALB/3T3 FBs (ATCC) were previously grown in cell culture plates and subsequently applied to the EHPGLS with DMEM containing 10% fetal bovine serum (FBS), 1% L-glutamine and 1% antibiotic. The EHPGLS samples were stored in duplicate in 12 well plates and sterilized

by gamma rays from  $^{60}\text{Co}$  (25 kGy) at room temperature (25 °C). After this step, the culture DMEM medium was applied for conditioning the EHPGLS samples for 20 min.

The FBs were cultured at a concentration of  $1.0 \times 10^4$  cells/cm<sup>2</sup> on EHPGLS with the aid of a stainless steel ring of 1 cm in diameter, thus defining the area of cell application. After 48 h, the rings were removed and DMEM culture medium (10% FBS, 1% L-glutamine, 1% antibiotic/antimitotic) was changed. After 96 h of fibroblasts cultivation, the EHPGLS samples were washed four times with phosphate buffered saline (PBS) pH 7.4. The EHPGLS were immersed in 0.9% saline for 15 min and then added glutaraldehyde 2.5 wt.% in water for 10 min for fixation. Then, the EHPGLS were washed four times with PBS pH 7.4 and lyophilized.

### 2.7. Statistical analysis

Analysis of variance (ANOVA) was applied on the results and the Tukey test was used to evaluate average differences (at a 95% of confidence interval).

## 3. Results and discussion

### 3.1. SEM characterization of EHPGLS

A major component of most biological tissues is the ECM with their fibrous structure that acts regulating almost all cellular behavior that is of critical importance for tissue engineering such as cell adhesion, migration, proliferation and differentiation [49–50].

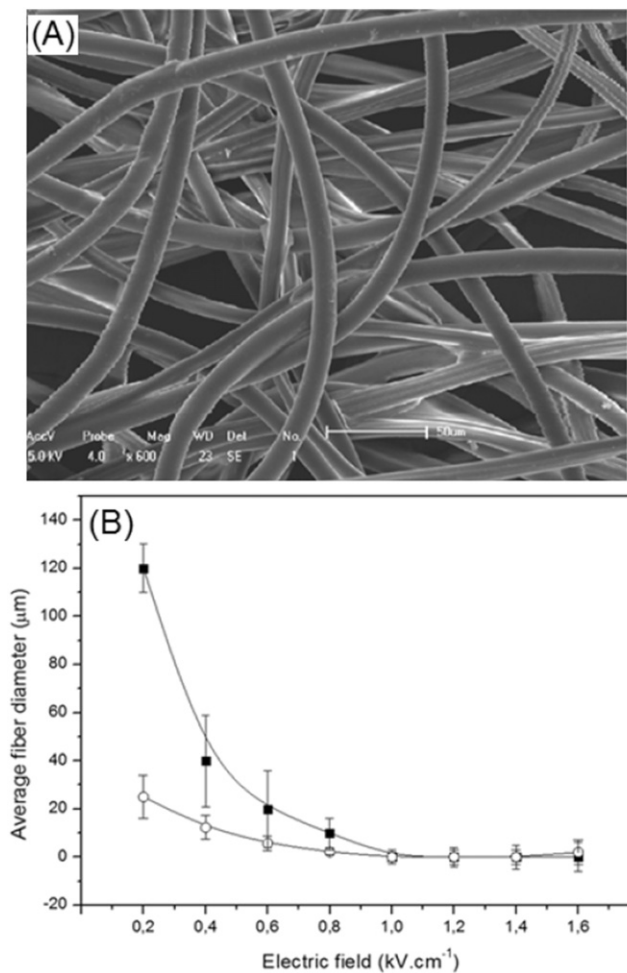


**Fig. 1.** SEM micrographs (A) and the effect of electric field and HPGL concentration on the measured average diameter of EHPGLS (B). HPGL concentration: 50 wt% (○) and 30 wt% (■) in 50:50 v/v methanol/DMF solution.

Through electrospinning technique HPGL can be engineered as ECM mimicking scaffolding systems for tissue engineering applications to simulate the organization of ECM. A typical SEM image of EHPGLS is shown in Fig. 1 (A). The images obtained from SEM were studied for the effect of the polymer concentration and electric field on fiber diameter and its distribution. Fig. 1(B) shows the effect of the electrical field on the measured average fiber diameter of the fibers at two different concentrations of the HPGL solution. It is evident from the Fig. 1 that increases the electrical field at all concentrations, the average diameter of the EHPGLS fibers decreases. The high electrical field can increase the electrostatic repulsive force on the charged HPGLS jet, thus favoring the narrowing of fiber diameter.

### 3.2. Effect of GMA concentration on crosslinking

It is well known that the porous architecture plays a critical role in improving the efficiency of polymer scaffolds in tissue engineering since the network structure of the pores promotes the guiding and new tissue formation [51–52]. The effect of GMA concentration on morphology of EHPGLS was characterized by using SEM and the results are shown in Fig. 2. It is evident that by increasing GMA contents on EHPGLS, porosity increases. The porosity of EHPGLS varied from  $65.2 \pm 1.8\%$  (when produced with 2.5% GMA) to  $89.3 \pm 4.2\%$  when produced with 20% of GMA (Fig. 2). These phenomena can be explained in terms of the compatibility of the GMA chains with the HPGL structure considering their solubility parameters ( $\delta$ ). The lower the difference between solubility parameters of PGMA and HPGL, a higher affinity between these two polymeric chains are expected. The solubility parameters for PGMA and HPGL are  $19.6 \text{ (MPa)}^{1/2}$  and  $24.5\text{--}26.6 \text{ (MPa)}^{1/2}$ , respectively [53–54]. The increases in porosity of EHPGLS with GMA

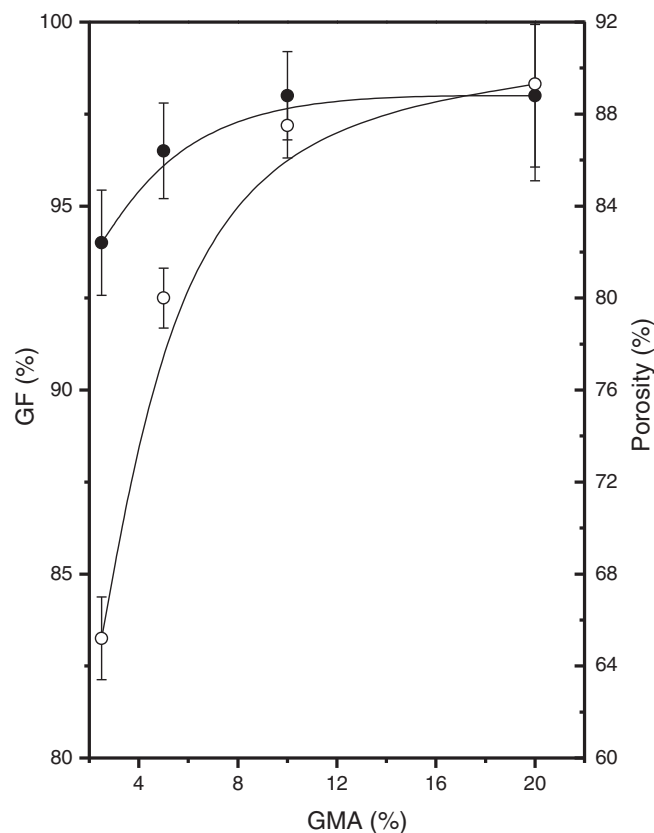


**Fig. 2.** Effect of GMA concentration (% w/w) on the porosity (○) and gel fraction (GF) (●) of electrospun HPGL scaffolds.

concentration may be due to the in situ formation of a heterogeneous structure resultant from the phase separation of HPGL and PGMA chains during crosslinking. These findings indicate that the porosity can be tuned by selecting the degree of GMA in EHPGLS.

### 3.3. Effect of GMA content on the gel fraction and swelling properties of EHPGLS

Fig. 2 show the effects of the crosslinking agent (GMA) concentration on the gel fraction (GF) of different formulations of EHPGLS. The GF quantifies the success of the GMA reaction crosslinking while indicating the migration of the uncrosslinking HPGL in water. All the synthesized EHPGLS are characterized by remarkably high GF values, even for the smallest concentration of the GMA. The values of GF are ranging between  $94 \pm 2.43\%$  for GMA concentration at 2.5% (w/w) and  $98 \pm 1.94\%$  for GMA concentration of 20% (w/w), respectively. As the concentration of crosslinking agent increases, there will be more crosslinking so the GF will increase.

The crosslinking with GMA is necessary to form a hydrogel in order to prevent dissolution of the hydrophilic HPGL chains in an aqueous environment. As shown in Fig. 3, as the concentration of the GMA was increased, the water absorbency (EWC) of the EHPGLS was decreased clearly indicating that a higher concentration of crosslinked chains generates an additional network with high crosslinking density [55]. Therefore, the network space gets diminished, and less water enters the EHPGLS.

The effects of GMA concentration on the EWC and water diffusion coefficient (D) are shown in Fig. 3. Here a clear picture is seen that both, EWC and D decreased as the amount of GMA was increased. This is due to the fact that as the concentration of GMA was increased,

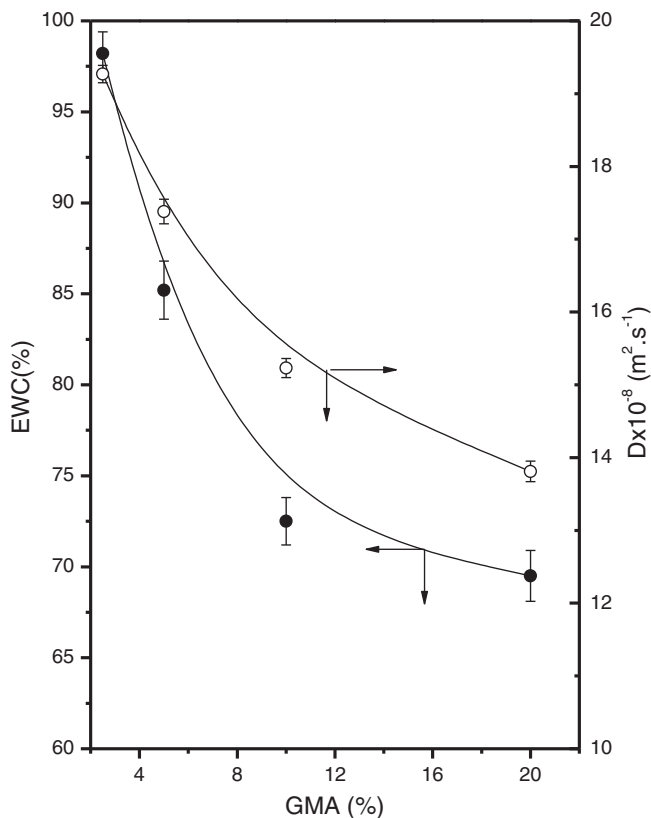


Fig. 3. Influence of GMA concentration on the EWC and water diffusion coefficient (D) properties of EHPGLS. The EWC (●) and D (○) measurements were made after EHPGLS immersion in PBS solution pH 7.4 at 37 °C.

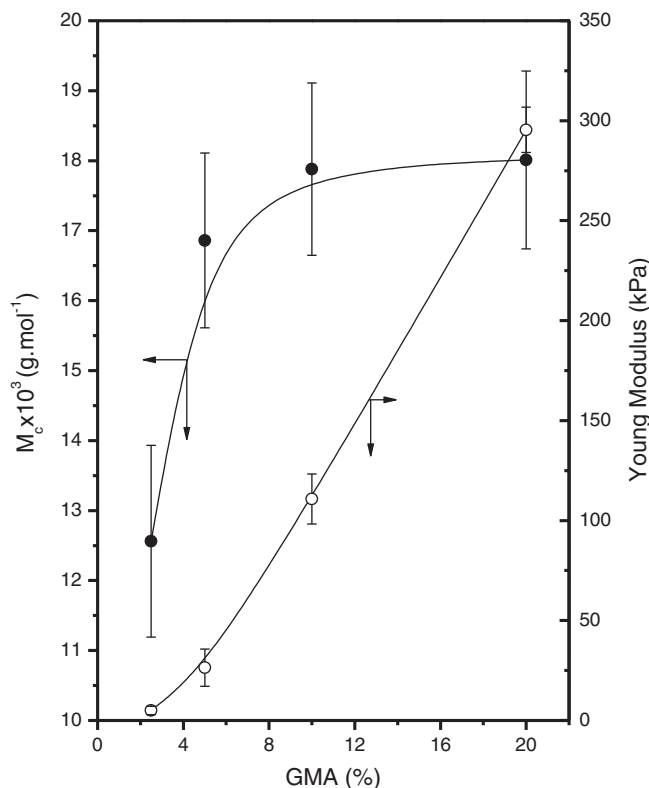


Fig. 4. Effect of GMA concentration on Young modulus (○) and  $M_c$  (●) for swollen (PBS solution pH 7.4 at 37 °C) EHPGLS.

there was a decrease in the mobility of the HPGL chain and the stability of the polymeric network was increased which resulted in a hindered HPGL structure with low swelling values as compared to samples with low degree of crosslinking [56–57].

### 3.4. Mechanical properties

The understanding of EHPGLS mechanical properties is very important for evaluating the feasibility of the material for the clinical applica-

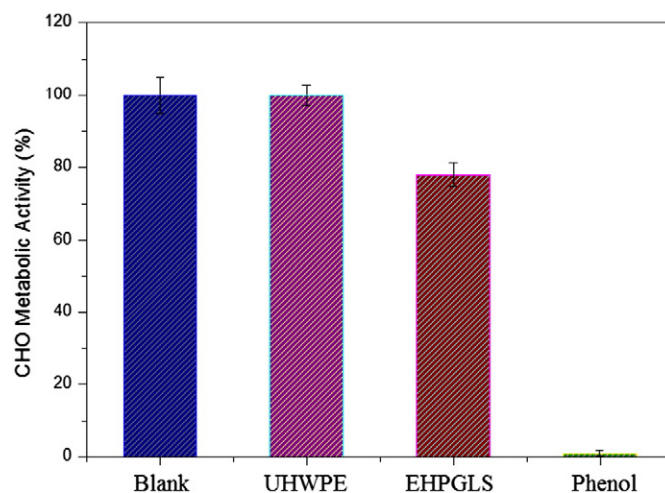


Fig. 5. CHO metabolic activity (extract) of EHPGLS. CHO cell populations were cultured in monolayer with extract media of UHWPE (negative control), phenol 0.3% (m/v) in PBS pH 7.4 (positive, cytotoxic control), EHPGLS or nothing (Blank).

tions in tissue engineering. In addition, in order to tailor the EHPGLS properties to meet the adequate specification for clinical applications in tissue engineering, a quantitative structure-property relationship of EHPGLS could be necessary [58–59]. The EHPGLS in their swollen state can be considered as an elastomer and the rubber elasticity theory can be used to the analysis of the relationship between the mechanical behavior and the polymer structure.

Considering an affine deformation model of the EHPGLS network in which electrospun fibers do not interact with each other but are treated as a collection of independent units, the molecular weight between crosslinks ( $M_c$ ) was calculated through Eq. (6) [60–61]:

$$M_c = 3 \frac{\rho RT}{E} \sqrt[3]{\phi} \quad (6)$$

where  $E$  is the Young's modulus,  $R$  is the gas constant,  $T$  is the absolute temperature,  $\rho$  is the polymer density and  $\phi$  is the equilibrium volume fraction of polymer in the swollen state.

For qualify EHPGLS for soft tissue engineering applications, they need to be flexible and sustain a sufficient mechanical [62]. Hence,

high elasticity (expressed through Young's Modulus) is the desirable mechanical properties of EHPGLS for soft tissue applications. The Young's modulus (YM) of EHPGLS samples as a function of the GMA concentration is shown in Fig. 4. It can be seen (Fig. 4) that the Young's modulus of EHPGLS samples increased linearly ( $r^2 = 0.997$ ) with increasing GMA concentration due to the increased crosslinking density. EHPGLS containing 20% (w/w) GMA concentration possessed highest tensile strength ( $295.4 \pm 11.32$  kPa) and was similar to the value reported by literature for the elastic modulus of human skin [63]. This value was approximately 58 times higher than that of non-crosslinked EHPGLS ( $5.1 \pm 2.12$  kPa).

An important parameter that was used to characterize the EHPGLS network is the molecular weight of the polymer chain between two neighboring crosslinks ( $M_c$ ).  $M_c$  is a measure of the degree of crosslinking of the polymer, regardless of the nature (physical or chemical) crosslinking. The molecular weights between the crosslinks are shown in Fig. 4. As can be seen (Fig. 4) by increasing molar percent of GMA (i.e. lightly to highly crosslinked) the number of efficient crosslinks per unit volume increase what appears to provide a  $M_c$  crosslinks increase.

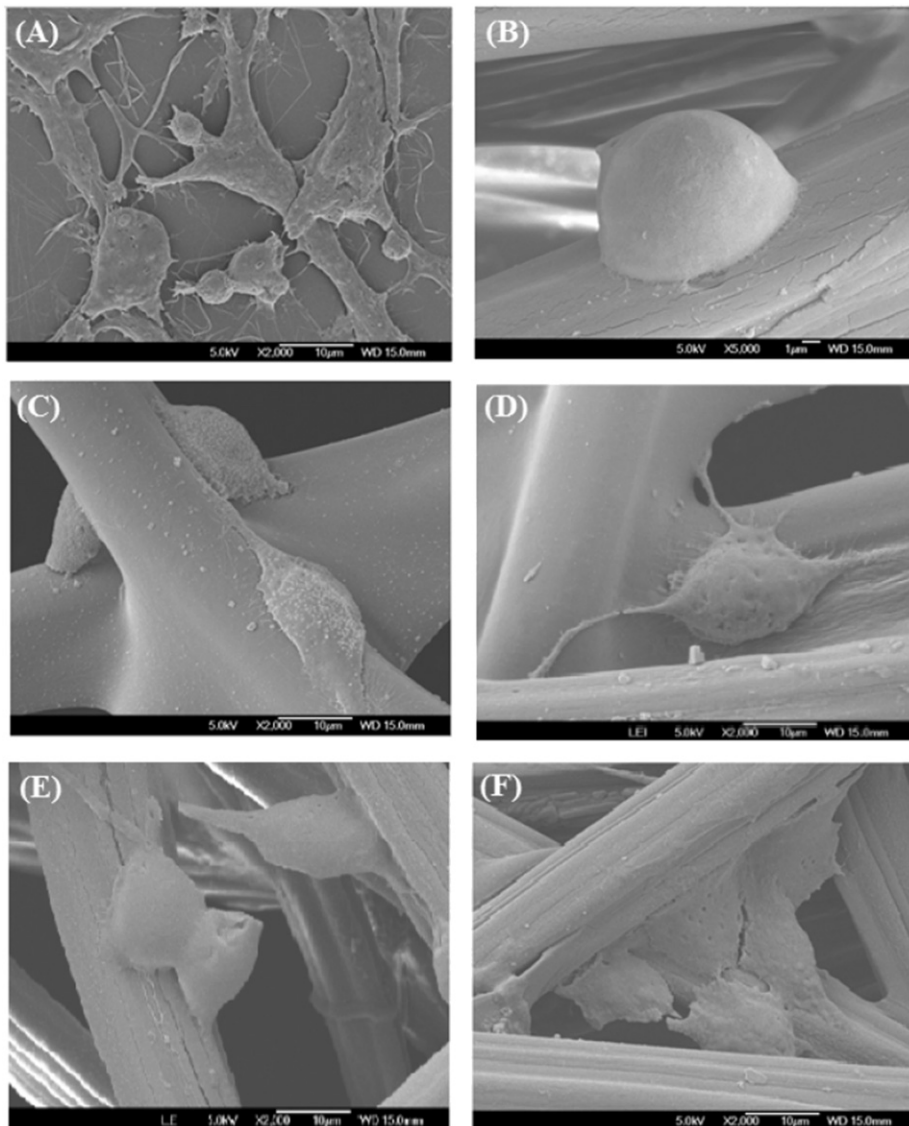


**Fig. 6.** Scanning electron microscopy (SEM) images of BALB/3T3 cells cultured in vitro on EHPGLS: control (A), after 24 h of cultures (B–D) and after 48 h of cultures (E–F). Magnification:  $\times 2000$  (A),  $\times 5000$  (B),  $\times 2000$  (C–F).

### 3.5. Effect of EHPGLS on CHO-K1 viability

The functionalization of HPGL with glycidyl methacrylate (GMA) was a strategy used in this work for producing HPGL-macromers to generate photo-crosslinkable electrospun scaffolds. These highly cross-linked EHPGLS with improved mechanical properties appear to be very attractive for soft tissue engineering applications and could expand the range of properties of crosslinked HPGL. However, the presence of unreacted GMA in EHPGLS can induce severe adverse biological effects [64].

Fig. 5 represents the cell viability of CHO cells after incubation for 24 h with EHPGLS extracts at various concentrations. The HDPE extracts (Fig. 5) did not have any significant cytotoxic effect on CHO cell lines in all the studied dilutions. However, in the CHO cells treated with increasing concentrations of phenol (Fig. 5), the cell viability was remarkably decreased in a dose-dependent manner. The  $IC_{50}$  value (%) of phenol against CHO cells was found to be 0% (Fig. 5). The  $IC_{50}$  of EHPGLS showed large values (80%), indicating higher cell compatibility implying that the electrospun scaffold has the potential to be applied in bio-applications. The results of the experiments based on indirect cytotoxicity assays indicate that EHPGLS exhibited negligible or no contamination with cytotoxic leachable for the mammalian cell line.

### 3.6. Cell adhesion and proliferation

In construction of scaffolds for tissue engineering the main strategy for modulating the cell-material interactions will be the creation of the mimetic biological surface that will be favorable to the adhesion and proliferation of cells [65]. In this study, BALB/3T3 cells were seeded to EHPGLS and cultured for 2 days. It is well known that the higher the number of viable cells attached to the surface, the better the biocompatibility of the scaffold [66].

The SEM observations of the adhesion and growth of BALB/3T3 cells fibroblasts were presented in Fig. 6. Fig. 6(A) shows the SEM micrographs of the FBs control cells. In Fig. 6(B), the FBs cells on the EHPGLS in the initial phase of adhesion are observed with their characteristic rounded shape, representing the cytoplasm concentrated in the spherical shape of the cell. After the initial stage of FBs adhesion the cytoplasmic projections are observed, losing their initial spherical shape. The formation of the first extensions of the cytoplasm and the scattering cytoplasm with a larger number of lateral projections were observed, suggesting that FBs has to begin the anchoring process in EHPGLS (Fig. 6(C, D)). Finally, the adhesion process is then completed and FBs showed spindle-like shape morphology and the cytoplasm occupies the maximum space in the EHPGLS, allowing neighboring cells to interact with each other as displayed in Fig. 6(E, F).

Today, it is well known that the cell adhesion process is caused by the change in the cytoplasm which tends to extend, retaining its initial volume and occupying the maximum space, as shown in Fig. 6(C-F). This cytoplasm extension is related to the presence of a set of integrin receptors responsible for the binding of substrate to the cytoskeleton [67]. At this step, the glycoproteins of the cell membrane are adsorbed to the surface and the cell deformation takes place while it tries to occupy the largest possible area [68–69]. In this work, it was observed that the frequency at which the FBs adhesion is increased as cell spreads (results not shown here). This fact could be associated with the fact that the more extended FBs cells with larger surfaces are (Fig. 6(E, F)), the greater the number of growth-factors molecules and nutrients they can capture [70].

## 4. Conclusions

In the present study, HPGL derived scaffolds were prepared by electrospinning and its properties including morphological, mechanical and biological behavior, were investigated. The prepared EHPGLS showed highly randomly fibrous morphology with diameter dependent

of the applied electrical field. The GMA crosslinking was sufficient to impart a mechanical integrity similar to soft tissues. The cytotoxicity study indicates that electrospun EHPGLS did not induce toxic effects on the CHO cells exhibiting high cell viability. The BALB/3T3 fibroblasts responded favorably to EHPGLS. The EHPGLS did not affect significantly the cell proliferation, which showed a significant increase over time. In conclusion, EHPGLS is an attractive biomaterial candidate for further studies in tissue engineering of soft tissues designing clinical strategies that could benefit the regenerative medicine

## Acknowledgments

This work was supported by financial supports of CNPq (305894/2014-5), CAPES, FINEP and FAPEMIG.

## References

- [1] M. Jafari, Z. Paknejad, M.R. Rad, S.R. Motamedian, M.J. Eghbal, N. Nadjmi, A. Khojasteh, Polymeric scaffolds in tissue engineering: a literature review, *J. Biomed. Mater. Res. B Appl. Biomater.* (2015), <http://dx.doi.org/10.1002/jbm.b.33547>.
- [2] F. Khan, M. Tanaka, S.R. Ahmad, Fabrication of polymeric biomaterials: a strategy for tissue engineering and medical devices (review), *J. Mater. Chem. B* 3 (2015) 8224–8249.
- [3] X. Duan, H. Sheardown, Dendrimer crosslinked collagen as a corneal tissue engineering scaffold: mechanical properties and corneal epithelial cell interactions, *Biomaterials* 27 (2006) 4608–4617.
- [4] J.M. Oliveira, R.A. Souza, N. Kotobuki, M. Tadokoro, M. Hirose, J.J. Mano, R.L. Reis, H. Oghushi, The osteogenic differentiation of rat bone marrow stromal cells cultured with dexamethasone-loaded carboxymethylchitosan/poly(amidoamine) dendrimer nanoparticles, *Biomaterials* 30 (2009) 804–813.
- [5] X. Zhang, Y. Li, Y.E. Chen, J. Chen, P.X. Ma, Cell-free 3D scaffold with two-stage delivery of miRNA-26a to regenerate critical-sized bone defects, *Nat. Commun.* 7 (2016) 1–32.
- [6] G. Mihov, D. Grebel-Koehler, A. Lubbert, G.W. Vandermeulen, A. Herrmann, H.A. Klok, K. Mullen, Polyphenylene dendrimers as scaffolds for shape-persistent multiple peptide conjugates, *Bioconjug. Chem.* 16 (2005) 283–293.
- [7] N. Joshi, M. Grinstaff, Applications of dendrimers in tissue engineering, *Curr. Top. Med. Chem.* 8 (2008) 1225–1236.
- [8] X. Duan, H. Sheardown, Dendrimer crosslinked collagen as a corneal tissue engineering scaffold: mechanical properties and corneal epithelial cell interactions, *Biomaterials* 27 (2006) 4608–4617.
- [9] M.A. Prince, H. Sheardown, Heparin-modified dendrimer cross-linked collagen matrices for the delivery of basic fibroblast growth factor (FGF-2), *J. Biomater. Sci. Polym. Ed.* 19 (2008) 1201–1218.
- [10] P.J. Geutjes, W.F. Daamen, P. Buma, W.F. Feitz, K.A. Faraj, T.H. van Kuppevelt, From molecules to matrix: construction and evaluation of molecularly defined bioscaffolds, *Adv. Exp. Med. Biol.* 285 (2006) 279–295.
- [11] S.H. Sontjens, D.L. Nettles, M.A. Carnahan, L.A. Setton, M.W. Grinstaff, Biodendrimer-based hydrogel scaffolds for cartilage tissue repair, *Biomacromolecules* 7 (2006) 310–316.
- [12] A.N. Santos, D.A.W. Soares, A.A.A. de Queiroz, Low potential stable glucose detection at dendrimers modified polyaniline nanotubes, *Mater. Res.* 13 (2010) 5–10.
- [13] A.A.A. de Queiroz, J.C. Bressiani, A.H.A. Bressiani, O.Z. Higa, G.A. Abraham, A novel bone scaffolds based on hyperbranched polyglycerol fibers filled with hydroxyapatite nanoparticles: in vitro cell response, *Key Eng. Mater.* 396–398 (2009) 633–636.
- [14] H.A.M. Faria, O.Z. Higa, A.A.A. de Queiroz, Polyglycerol dendrimers immobilized on radiation grafted poly-HEMA hydrogels: surface chemistry characterization and cell adhesion, *Radiat. Phys. Chem.* 98 (2014) 118–123.
- [15] A.A.A. De Queiroz, E.G.R. Fernandes, G.A. Abraham, J. San-Roman, Antithrombotic properties of bioconjugate streptokinase-polyglycerol dendrimers, *J. Mater. Sci. Mater. Med.* 17 (2006) 105–111.
- [16] W.-J. Li, C.T. Laurencin, E.J. Caterson, R.S. Tuan, F.K. Ko, Electrospun nanofibrous structure: a novel scaffold for tissue engineering, *J. Biomed. Mater. Res.* 60 (2002) 613–621.
- [17] A. Hasan, A. Memic, N. Annabi, M. Hossain, A. Paul, M.R. Dokmeci, F. Dehghani, A. Khademhosseini, Electrospun scaffolds for tissue engineering of vascular grafts, *Acta Biomater.* 10 (2014) 11–25.
- [18] M.M. Hohman, M. Shin, G. Rutledge, M.P. Brenner, Electrospinning and electrically forced jets. I. Stability theory, *Phys. Fluids* 13 (2001) 2201–2220.
- [19] D.H. Reneker, A.L. Yarin, H. Fong, S. Koombhongse, Bending instability of electrically charged liquid jets of polymer solutions in electrospinning, *J. Appl. Phys.* 87 (2000) 4531–4547.
- [20] A.A.A. de Queiroz, N.C.V. Baracho, E.A.T. Vargas, J. Brito, Hyperbranched polyglycerol electrospun nanofibers for wound dressing applications, *Acta Biomater.* 6 (2010) 1069–1078.
- [21] H. Pan, H. Jiang, W. Chen, Interaction of dermal fibroblasts with electrospun composite polymer scaffolds prepared from dextran and poly lactide-coglycolide, *Biomaterials* 27 (2006) 3209–3220.
- [22] S. Agarwal, J.H. Wendorff, A. Greiner, Use of electrospinning technique for biomedical applications, *Polymer* 49 (2008) 5603–5621.

- [23] A. Welle, M. Kroger, M. Doring, K. Niederer, E. Pindel, I.S. Chronakis, Electrospun aliphatic polycarbonates as tailored tissue scaffold materials, *Biomaterials* 28 (2007) 2211–2219.
- [24] J.P.E. Junker, P. Sommar, M. Skog, H. Johnson, G. Kratz, Adipogenic, chondrogenic and osteogenic differentiation of human dermal fibroblasts, *Cells Tissues Organs* 191 (2010) 105–118.
- [25] T. Wong, J.A. McGrath, H. Navsaria, The role of fibroblasts in tissue engineering and regeneration, *Br. J. Dermatol.* 156 (2007) 1149–1155.
- [26] I. Jones, L. Currie, R. Martin, A guide to biological skin substitutes, *Br. J. Plast. Surg.* 55 (2002) 185–193.
- [27] P.P. Bonvallet, M.J. Schultz, E.H. Mitchell, J.L. Bain, B.K. Culpepper, S.J. Thomas, S.L. Bellis, Microporous dermal-mimetic electrospun scaffolds pre-seeded with fibroblasts promote tissue regeneration in full-thickness skin wounds, *PLoS One* 10 (2015), e0122359.
- [28] D. Revi, W. Paul, A.T.V. Anilkumar, C.P. Sharma, Chitosan scaffold co cultured with keratinocyte and fibroblast heals full thickness skin wounds in rabbit, *J. Biomed. Mater. Res. A* 102 (2014) 3273–3281.
- [29] J. Mansbridge, Commercial considerations in tissue engineering, *J. Anat.* 209 (2006) 527–532.
- [30] S. MacNeil, Progress and opportunities for tissue-engineered skin, *Nature* 445 (2007) 874–880.
- [31] G.K. Naughton, From lab bench to market: critical issues in tissue engineering, *Ann. N. Y. Acad. Sci.* 961 (2002) 372–385.
- [32] J.D. Raguse, H.J. Gath, A metabolically active dermal replacement (Dermagraft) for vestibuloplasty, *J. Oral Rehabil.* 32 (2005) 337–340.
- [33] A.R. Chandrasekaran, J. Venugopal, S. Sundarajan, S. Ramakrishna, Fabrication of a nanofibrous scaffold with improved bioactivity for culture of human dermal fibroblasts for skin regeneration, *Biomed. Mater.* 6 (2011) 1–10.
- [34] Q.L. Loh, C. Choong, Three-dimensional scaffolds for tissue engineering applications: role of porosity and pore size, *Tissue Eng. B Rev.* 19 (2013) 485–502.
- [35] D.E. Discher, P. Janmey, Y.L. Wang, Tissue cells feel and respond to the stiffness of their substrate, *Science* 310 (2005) 1139–1143.
- [36] M.H. Zaman, L.M. Trapani, A.L. Sieminski, D. Mackellar, H. Gong, R.D. Kamm, A. Wells, D.A. Lauffenburger, P. Matsudaira, Migration of tumor cells in 3D matrices is governed by matrix stiffness along with cell-matrix adhesion and proteolysis, *Proc. Natl. Acad. Sci. U. S. A.* 103 (2006) 10889–10894.
- [37] M.H. Zaman, R.D. Kamm, P. Matsudaira, D.A. Lauffenburger, Computational model for cell migration in three-dimensional matrices, *Biophys. J.* 89 (2005) 1389–1397.
- [38] S.J. Hollister, R.D. Maddox, J.M. Taboas, Optimal design and fabrication of scaffolds to mimic tissue properties and satisfy biological constraints, *Biomaterials* 23 (2003) 4095–4103.
- [39] W. Sun, A. Darling, B. Starly, J. Nam, Computer aided tissue engineering: overview, scope and challenges, *J. Biotechnol. Appl. Biochem.* 39 (2004) 29–47.
- [40] Z. Fang, B. Starly, W. Sun, Computer-aided characterization for effective mechanical properties of porous tissue scaffolds, *Comput. Aided Des.* 37 (2005) 65–72.
- [41] A. Tiwari, J.J. Grailer, S. Pilla, D.A. Steeber, S. Gong, Biodegradable hydrogels based on novel photopolymerizable guar gum-methacrylate macromonomers for in situ fabrication of tissue engineering scaffolds, *Acta Biomater.* 5 (2009) 3441–3452.
- [42] G. Rokicki, P. Rakoczy, P. Parzuchowski, M. Sobiecki, Hyperbranched aliphatic polyethers obtained from environmentally benign monomer: glycerol carbonate, *Green Chem.* 7 (2005) 529–539.
- [43] S.S. Sreedhara, N.R. Tata, A novel method for measurement of porosity in nanofiber materials using pycnometer in filtration, *J. Eng. Fibers Fabr.* 8 (2013) 132–137.
- [44] N. Nagasawa, T. Yagi, T. Kume, F. Yoshii, Radiation crosslinking of carboxymethyl starch, *Carbohydr. Polym.* 58 (2004) 109–113.
- [45] M. Arnal-Pastor, C.M. Ramos, M.P. Garnés, M.M. Pradas, A.V. Lluch, Electrospun adherent-antiadherent bilayered membranes based on cross-linked hyaluronic acid for advanced tissue engineering applications, *Mater. Sci. Eng. C* 33 (2013) 4086–4093.
- [46] J. Crank, *The Mathematics of Diffusion*, Clarendon Press, Oxford (England), 1975 244.
- [47] ASTM Standard D882-09 (2009). Standard Test Method for Tensile Properties of Thin Plastic Sheeting, ASTM International, West Conshohocken, PA, www.astm.org/Standards.
- [48] ISO, Biological Evaluation of Medical Devices Part 5: Tests for In Vitro Cytotoxicity, 2009, International Organization for Standardization, Geneva, Switzerland, 2009 10993–10995.
- [49] R.O. Hynes, The extracellular matrix: not just pretty fibrils, *Science* 326 (2009) 1216–1219.
- [50] W.P. Daley, S.B. Peters, M. Larsen, Extracellular matrix dynamics in development and regenerative medicine, *J. Cell Sci.* 121 (2008) 255–264.
- [51] Q.L. Loh, C. Choong, Three-dimensional scaffolds for tissue engineering applications: role of porosity and pore size, *Tissue Eng. B Rev.* 19 (2013) 485–502.
- [52] S.J. Hollister, Porous scaffold design for tissue engineering, *Nat. Mater.* 4 (2005) 518–524.
- [53] K.W. Lee, J.W. Chung, S.-Y. Kwak, Synthesis and characterization of bio-based alkyl terminal hyperbranched polyglycerols: a detailed study of their plasticization effect and migration resistance, *Green Chem.* 18 (2016) 999–1009.
- [54] V. Bliznyuk, Y. Galabura, R. Burtovyvy, P. Karagani, N. Lavrikk, I. Luzinov, Electrical conductivity of insulating polymer nanoscale layers: environmental effects, *Phys. Chem. Chem. Phys.* 16 (2014) 1977–1986.
- [55] C.C. Lin, A.T. Metters, Hydrogels in controlled release formulations: network design and mathematical modeling, *Adv. Drug Deliv. Rev.* 58 (2006) 1379–1408.
- [56] R.S.H. Wong, M. Ashton, K. Dodou, Effect of crosslinking agent concentration on the properties of unmedicated hydrogels, *Pharmaceutics* 7 (2015) 305–319.
- [57] N.A. Peppas, Y. Huang, M. Torres-Lugo, J.H. Ward, J. Zhang, Physicochemical foundations and structural design of hydrogels in medicine and biology, *Annu. Rev. Biomed. Eng.* 2 (2000) 9–29.
- [58] D.E. Discher, P. Janmey, Y.L. Wang, Tissue cells feel and respond to the stiffness of their substrate, *Science* 310 (2005) 1139–1143.
- [59] A.J. Engler, S. Sen, H.L. Sweeney, D.E. Discher, Matrix elasticity directs stem cell lineage specification, *Cell* 126 (2006) 677–689.
- [60] N.A. Peppas, J.Z. Hilt, A. Khademhosseini, R. Langer, Hydrogels in biology and medicine: from molecular principles to bionanotechnology, *Adv. Mater.* 18 (2006) 1345–1360.
- [61] T. Stylianopoulos, C.A. Bashur, A.S. Goldstein, S.A. Guelcher, V.H. Barocas, Computational predictions of the tensile properties of electrospun fiber meshes: effect of fiber diameter and fiber orientation, *J. Mech. Behav. Biomed. Mater.* 1 (2008) 326–335.
- [62] H.S. Kim, J.H. Kim, J.O. Kim, S. Ku, H. Cho, D. Han, P. Huh, Fabrication of poly(ethylene oxide) hydrogels for wound dressing application using E-beam, *Macromol. Res.* 22 (2014) 131–138.
- [63] X. Liang, S.A. Boppart, Biomechanical properties of in vivo human skin from dynamic optical coherence elastography, *IEEE Trans. Biomed. Eng.* 57 (2010) 953–959.
- [64] T. Poplawski, E. Pawlowska, M. Wisniewska-Jarosinska, D. Ksiazek, J. Szczepanska, J. Blasiak, Cytotoxicity and genotoxicity of glycidyl methacrylate, *Chem. Biol. Interact.* 180 (2009) 69–78.
- [65] Y.Z. Zhang, B. Su, J. Venugopal, S. Ramakrishna, C.T. Lim, Biomimetic and bioactive nanofibrous scaffolds from electrospun composite nanofibers, *Int. J. Nanomedicine* 2 (2007) 623–638.
- [66] P. Thevenot, W. Hu, L. Tang, Surface chemistry influence implant biocompatibility, *Curr. Top. Med. Chem.* 8 (2008) 270–280.
- [67] P. Moreno-Layseca, C. Streuli, Mini review signaling pathways linking integrin's with cell cycle progression, *Matrix Biol.* 34 (2014) 144–153.
- [68] M. Steinberg, Differential adhesion in morphogenesis: a modern view, *Curr. Opin. Genet. Dev.* 17 (2007) 281–286.
- [69] R. Tzoneva, N. Faucheux, T. Groth, Wettability of substrata controls cell-substrate and cell-cell adhesions, *Biochim. Biophys. Acta* 1770 (2007) 1538–1547.
- [70] E.A. Cavalcanti-Adam, T.V.A. Micoulet, H. Kessler, B. Geiger, J.P. Spatz, Cell spreading and focal adhesion dynamics are regulated by spacing of integrin ligands, *Biophys. J.* 92 (2007) 2964–2974.